Available online at www.sciencedirect.com
ScienceDirect
Journal of Power Sources 159 (2006) 1162–1168
JOURNAL OF POWER SOURCES
www.elsevier.com/locate/jpowsour

Short communication

A strategy of estimating fuel concentration in a direct liquid-feed fuel cell system

Yu-Jen Chiu *, Hsin-Chung Lien

Department of Mechanical Engineering, Northern Taiwan Institute of Science and Technology, No. 2 Xueyuan Rd., Beitou District, Taipei City 11202, Taiwan, ROC

Received 19 November 2005; accepted 20 December 2005
Available online 18 April 2006

Abstract

Fuel control is one of the most pressing topics to achieve a self-sustainable direct liquid-feed fuel cell system, such as a direct methanol fuel cell (DMFC), and enhance its overall efficiency. In a DMFC system, sensing the methanol concentration generally serves as the basis of the fuel control strategies. This paper proposes a three-dimensional measurement space and *constant concentration surfaces* (CCS) to develop an algorithm of estimating fuel concentration in a liquid-feed system, which embraces the following merits: (1) it measures only three quantities or indices that correlate with the fuel concentration. The indices can be chosen as current, voltage, temperature, or other quantities that are easily acquired in an operating fuel cell system. The estimation can be accomplished without interrupting the operation of the system, (2) it estimates the fuel concentration in a three-dimensional measurement space; hence it is suitable for situations when one or more operating conditions are varying, (3) it can be performed as a sensor-less approach that requires no additional methanol sensors, thus consuming the less system power, and (4) it is particularly suitable for small and hand-held applications.

Keywords: Direct liquid-feed fuel cell; DMFC; Concentration sensor

1. Introduction

The direct methanol fuel cell (DMFC) is suitable for small or hand-held application systems like consumer electronics devices. In such applications, the mass, volume, and efficiency will be the most significant issues to be considered. However, the methanol crossover phenomenon in a DMFC has been a crucial limitation that may greatly reduce the efficiency of the system when methanol fuel of higher concentration is fed into the fuel cell units. On the other hand, to achieve a specified total energy delivery, introducing methanol fuel of lower concentration will lead to a lower energy density; and the system would be heavier and larger. To take the efficiency and energy density into account simultaneously, it is desirable to replenish a fuel cartridge with concentrated methanol fuel to increase the energy density of the system. Then the fuel is pre-diluted inside the fuel cell system to an adequate concentration level before being fed onto the fuel cell units (i.e. membrane electrode assemblies, MEAs), thus preventing excessive fuel crossover. Furthermore, fuel concentration is one of the most significant factors that dominate the behavior of a fuel cell. Hence it should be well controlled to achieve optimal performance in a fuel cell system. As a result, fuel concentration control is essential to meet the requirements. Techniques of sensing methanol concentration are therefore important to serve as the basis of fuel control strategies.

There have been various approaches to acquire the methanol concentration in a DMFC system. The approaches can be divided into two major categories. The first one correlates the concentration of the methanol aqueous solution with its physical properties, such as density, dielectric constant, ultrasound velocity, infrared absorptivity, optical behavior, transmittance, etc. [1–5]. However, this kind of approach requires more complex and delicate instruments that may not be suitable for small and hand-held applications under cost, mass, and volume constrain. The second category of methanol concentration sensing schemes is based on the electrochemical characteristics of the fuel cells themselves. They can further be divided into two types: galvanic type and electrolytic type. The former correlates the polarization curve [6], short circuit current [7], open circuit voltage [8], and even indirect measurement data [9,10] with the methanol con-

* Corresponding author. Tel.: +886 2 28927154x8011; fax: +886 2 28935295.
E-mail address: yjchiu@ntist.edu.tw (Y.-J. Chiu).

0378-7753/$ – see front matter © 2006 Elsevier B.V. All rights reserved.
doi:10.1016/j.jpowsour.2005.12.099

centration to be determined. These sensing schemes adopt the inherent behavior of a fuel cell and hence are simple, straightforward, and even sensor-less. However, they are very sensitive to the operational conditions such as temperature, voltage (or current density), and flow rate of the fuel (or air). Additional compensation is needed for situations that are varying. The electrolytic type sensing schemes measure the limiting current or the half-cell potential to establish the relationship with methanol concentration [11–15]. In these designs, a substantial sensor is required while the reactions wherein are not spontaneous. Additional external power input is required to drive the oxidation and reduction reactions on the anode and cathode sides, respectively. Temperature still plays a significant role and influences the measurement results.

The present paper proposes an estimation algorithm to determine methanol concentration in a small DMFC system. The method is based on a three-dimensional measurement space with the measurement dimensions being current, voltage, and temperature. Whenever other measurement quantities or indices can be correlated with the methanol concentration, they could also serve as the three measurement dimensions while the proposed algorithm is still valid. Since the method is performed in a three-dimensional measurement space, it is suitable for situations where one or more operating factors, like temperature or current density, are varying. Moreover, it can be designed as a sensor-less approach that consumes the less system power while minimizing the cost, mass, and volume of the system. Such a design is particularly beneficial for small and hand-held applications.

2. The estimation algorithm

The present paper proposes an Interpolation algorithm based on Constant Concentration Surfaces (ICCS algorithm) to estimate the fuel concentration in a liquid-feed fuel cell system. Its primary concept accompanying the solution schemes will be illustrated in this section.

2.1. The notion of ICCS algorithm

The polarization curve (*I–V* curve) reveals the most important characteristic of a fuel cell, which depicts the relation of voltage to current density. The relation can be briefly expressed as follows [16]:

$$V = E - (i + i_n)r - A \ln\left[\frac{i + i_n}{i_0}\right] + B \ln\left[1 - \frac{i + i_n}{i_l}\right] \quad (1)$$

where E denotes the reversible open circuit voltage, while V and i are voltage and current density, respectively. For a given direct methanol fuel cell, the values of the parameters A, B, i_0, i_n, i_l, and r in Eq. (1) closely depend on the operational at conditions including temperature, methanol concentration supplied to the anode, flow rates of the delivered fuel and air, and pressure built in the anode and cathode chambers. The delivery of fuel and air not only provides the reactants for the electrochemical reactions, but also removes the products and heat generated by the reactions. Accordingly, the effect of flow rates of fuel and air on Eq. (1) can be indirectly translated into effects on the temperature and fuel concentration. Moreover, the pressure effect can influence the mass transport or concentration. Generally, the pressure issue is omitted in a smaller-scaled DMFC system since only a limited energy budget is left for the balance of plant (BOP), which cannot offer enough power to build a much higher pressure for fuel and air delivery. As a result, whenever the flow rates of fuel and air are specified, the temperature and methanol concentration will be the most significant condition variables to be controlled. Then for a given DMFC, the behavior of the polarization curve in Eq. (1) can be written as

$$f(I, V, C, T) = 0 \quad (2)$$

where I, V, C and T denote current, voltage, fuel concentration, and operating temperature in order. One can observe that, in Eq. (2), three of the four variables are independent while the rest should be compliant with the equation. It represents the most important relationship between the material properties and system operating variables.

Generally speaking, the aforementioned operational variables should be confined within certain regions, e.g. 20–70 °C and 0.5–2.0 M for temperature and fuel concentration, respectively. Under such situations, the *I–V* curve of a DMFC will positively shift toward the higher performance region (higher voltage with fixed current or higher current with fixed voltage) whenever the operation temperature increases (adopting constant fuel concentration) or the fuel concentration increases (adopting constant operation temperature). Although the aforementioned qualitative tendency of the DMFC properties has been well known, it is still a complicated task to quantitatively determine the relationship described in Eq. (2).

Since three of the four variables in Eq. (2) are independent, this paper introduces a three-dimensional measurement space $\Re^3$ spanned by three measurement axes as its basis to estimate fuel concentration. In the case of Eq. (2), if the fuel concentration level is specified, say C_0, then a series of *I–V* curves can be acquired corresponding to various temperature levels. The *I–V* curves are depicted in a three-dimensional measurement space $\Re^3$ with its axes being current, voltage, and temperature. Moreover, a surface S spanned by these *I–V* curves can be obtained, as is shown in Fig. 1. Since all these *I–V* curves correspond to the same fuel concentration level C_0 and they will shift positively toward the higher performance region accompanying an increase of temperature, any other point on this surface S will also be correlated to C_0. Accordingly, such a surface is defined as a Constant Concentration Surface (CCS).

For an unknown fuel concentration level C_u, one can take an in situ measurement of current, voltage, and temperature of a fuel cell system then have a point P^+ (or P^-) located in the measurement space $\Re^3$, as was shown in Fig. 2. By judging how far the point P^+ (or P^-) is away from the surface S, it is inferred how large the concentration difference between C_u and C_0 is. Whenever two or more CCSs are pre-established with given fuel concentration levels, an Interpolation algorithm based on Constant Concentration Surfaces (ICCS) can then be adopted for estimating the unknown concentration level C_u, as will be

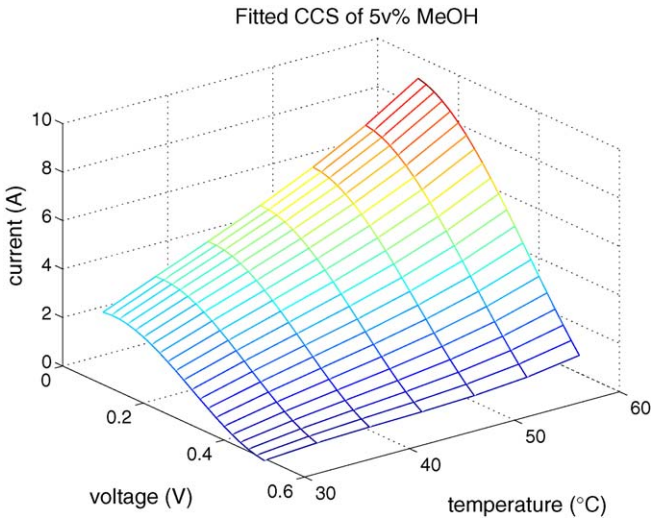

Fig. 1. A constant concentration surface in a three-dimensional measurement space $\Re^3$.

illustrated later. Consequently, the present paper depicts Eq. (2) by a graphical manner, meanwhile, gives a well estimation of fuel concentration in a liquid-feed fuel cell system.

2.2. The solution scheme of ICCS algorithm

The solution scheme of the ICCS algorithm can be divided into two stages, that is, establishment of CCSs and the interpolation procedure.

2.2.1. Establishment of CCSs

First, a number of CCSs are pre-established corresponding to specified fuel concentration levels. Each CCS is approximated by a cubic polynomial equation. Therefore, only 10 coefficients should be stored in the energy management system (EMS) instead of the whole experimental database, thus greatly enhancing its efficiency.

By confining a specified fuel concentration level C_k, a set of I–V curves can be obtained experimentally under various temperature levels and a CCS S_k is generated in $\Re^3$. The surface S_k is defined as follows

$$f_k(I, V, C, T)|_{C=C_k} \triangleq g_k(I, V, T) = 0 \tag{3}$$

For any combination of (I, V, T) that satisfies Eq. (3), it represents a point on the surface S_k corresponding to the same fuel concentration level C_k. In practice, let function g_k in Eq. (3) be approximated by a cubic polynomial as

$$\begin{aligned} g_k(I, V, T) = I - (&a_{1k} + a_{2k}T + a_{3k}V + a_{4k}T^2 + a_{5k}TV \\ &+ a_{6k}V^2 + a_{7k}T^3 + a_{8k}T^2V + a_{9k}TV^2 + a_{10k}V^3) \\ \equiv\ & 0 \end{aligned} \tag{4}$$

where $a_{1k}, a_{2k}, \ldots, a_{10k}$ are constant coefficients to be determined. One can take measurement (I_i, V_i, T_i) for $i = 1, 2, \ldots, m$ under various temperature and voltage (or current) levels and substitute all the values into Eq. (4) to have a set of polynomial equations consisting of unknown coefficients $a_{1k}, a_{2k}, \ldots, a_{10k}$:

$$\mathbf{g}_k = \begin{bmatrix} I_1 \\ I_2 \\ \vdots \\ I_m \end{bmatrix} \begin{bmatrix} 1 & T_1 & V_1 & T_1^2 & T_1V_1 & V_1^2 & T_1^3 & T_1^2V_1 & T_1V_1^2 & V_1^3 \\ 1 & T_2 & V_1 & T_2^2 & T_2V_2 & V_2^2 & T_2^3 & T_2^2V_2 & T_2V_2^2 & V_2^3 \\ \vdots & \vdots & \vdots & \vdots & \vdots & \vdots & \vdots & \vdots & \vdots & \vdots \\ 1 & T_m & V_m & T_m^2 & T_mV_m & V_m^2 & T_m^3 & T_m^2V_m & T_mV_m^2 & V_m^3 \end{bmatrix} \begin{bmatrix} a_{1k} \\ a_{2k} \\ \vdots \\ a_{10k} \end{bmatrix} \triangleq \mathbf{b} - \mathbf{M}\mathbf{a}_k \tag{5}$$

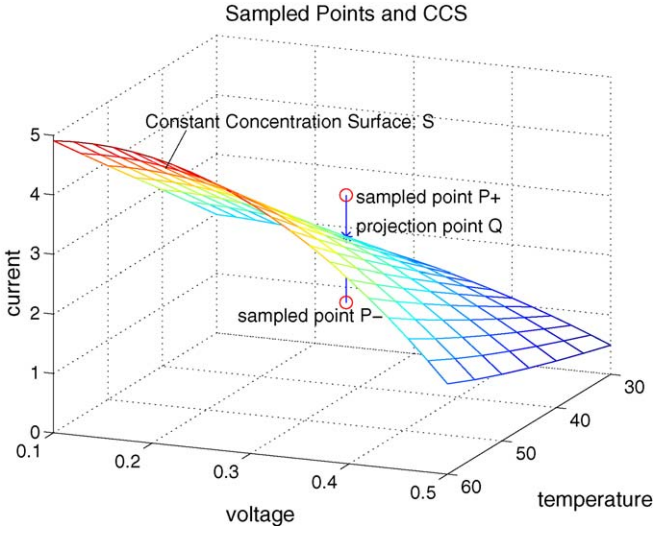

Fig. 2. A pre-established CCS and measurement points in $\Re^3$.

Then the well known Least-Squares Method can be adopted for solving $\mathbf{a}_k = [a_k, a_{1k}, a_{2k}, \ldots, a_{10k}]^{\mathrm{T}}$ in Eq. (5):

$$\mathbf{a}_k = (\mathbf{M}^{\mathrm{T}}\mathbf{M})^{-1}\mathbf{M}^{\mathrm{T}}\mathbf{b} \tag{6}$$

All the data acquisition and relevant computations can be performed beforehand, while only the values of a_k are necessary in the energy management system of a fuel cell system to represent a pre-established CCS of concentration C_k.

2.2.2. Interpolation procedure based on CCS

Let an arbitrarily point $P_u(I_u, V_u, T_u)$ in $\Re^3$ correspond to an unknown fuel concentration level C_u, where I_u, V_u, T_u are the measured current, voltage and temperature, in that order. Moreover, a number of CCSs S_k corresponding to the given methanol concentration levels C_k, for $k = 1, 2, \ldots, n$, are pre-established. The following illustration will transfer the relationship between $P_u(I_u, V_u, T_u)$ and S_k in $\Re^3$ into a current–concentration relation to have an interpolation formula.

Whenever a number of CCSs S_k and a measured point $P_u(I_u, V_u, T_u)$ are depicted in $\Re^3$, P_u will have n projection points Q_k

on S_k for $k = 1, 2, \ldots, n$ along the current axis. The projection point Q_k has a value of current I_k that can be interpreted as

$$I_k = a_{1k} + a_{2k}T_u + a_{3k}V_u + a_{4k}T_u^2 + a_{5k}T_uV_u + a_{6k}V_u^2 + a_{7k}T_u^3 + a_{8k}T_u^2V_u + a_{9k}T_uV_u^2 + a_{10k}V_u^3 \quad (7)$$

where V_u and T_u are the voltage and temperature of the measured point P_u, while a_{1k}, a_{2k}, K, a_{10k} are the coefficients of the pre-established CCS S_k of concentration C_k for $k = 1, 2, K, n$.

Then the unknown fuel concentration C_u can be determined by the Lagrange interpolation formula as follows [17]:

$$C_u = \sum_{k=1}^{n} \left(\prod_{\substack{j=1 \\ j \neq k}}^{n} \frac{I_u - I_j}{I_k - I_j} \right) C_k \quad (8)$$

where I_u is the current value of the measured point P_u, C_k denotes the fuel concentration of the pre-established SSCs, while I_j and I_k is determined by Eq. (7).

Accordingly, the ICCS algorithm has an in situ and unique estimation of the fuel concentration of a liquid-feed fuel cell system, merely by measuring the current, voltage and temperature that are all easily acquired throughout the operating region. One remark should be made that whenever other measurement quantities or indices can be correlated with the methanol concentration, they could also serve as the three measurement dimensions instead of current, voltage and temperature, and the proposed algorithm is still valid.

3. Experiments

The aforementioned ICCS algorithm is verified by experimental results based on standard testing procedures of a unit fuel cell. A standard testing module of a unit DMFC (with 50 mm × 50 mm MEA, DuPont Nation® 117) is adopted on a testing system (890B model of Scribner Associates Inc.) in the following experiments. The channel type of the graphite endplates is serpentine and 2 mm in width and depth. Four temperature levels and six concentration levels are considered in establishing CCSs, as are shown in Table 1. The methanol fuel is pre-heated to the desired temperature then delivered by a liquid pump and accompanying flow rate control. Moreover, a thermostat is attached to the testing module to control the operating temperature during the experiments. In order to keep the fuel concentration constant in each level, the fuel exhausted from the outlet of the testing module will not circulate back to the fuel reservoir. Furthermore, the flow rates of the methanol and air are kept constant to exclude the influence of heat exchange deviation. That would be 500 ml min^{-1} for air and 11.2 ml min^{-1} for the methanol solution (2A at 4× stoichiometric rate in 3% methanol fuel). For a given temperature and concentration, the electrical load is controlled under a constant voltage mode from 0.5 to 0.1 V with increments of −0.05 V. Meanwhile an *I–t* chart (current versus time) is recorded. There will be corresponding rising steps in the *I–t* charts whenever the voltage is downward regulated. The stabilized current values in each step are acquired for each voltage scan to have an *I–V* curve. For each concentration level, there will be four *I–V* curves of different temperature levels and 36 measured points of (I_i, V_i, T_i) in total, thus establishing the CCS by using Eqs. (5) and (6).

Table 1
A brief list of the experimental conditions

Items	Descriptions
1. MEA	50 mm × 50 mm (DuPont Nation® 117)
2. Graphite channel type	Serpentine, 2 mm in width and depth
3. Temperature levels (°C)	30, 40, 50, 60
4. Fuel concentration levels for pre-established CCSs (vol.%)	3, 4, 5, 6, 8, 10
5. Fuel concentration levels for verification points (vol.%)	3.5, 4.5, 5.5
6. Fixed air flow rate (ml min^{-1})	500
7. Fixed fuel flow rate	11.2 ml min^{-1} (2A at 4× stoichiometric rate in 3 vol.% fuel)
8. Electrical load	Scanned under constant voltage mode from 0.5 to 0.1 V with an increment of −0.05 V

The following experimental evaluation consists of three parts: (1) concept validation of CCS, (2) establishment of CCSs and feasible measurement regions, and (3) evaluation of ICCS algorithm.

4. Results and discussions

4.1. Concept validation of CCS

Before proceeding with further evaluation, the concept of CCS is first validated. Four *I–V* curves of different temperature levels listed in Table 1 are acquired based on 5 vol.% concentration. Then the constant coefficients, denoted by a_5, can be solved by Eqs. (5) and (6), thus establishing a CCS named S_5. Afterwards 16 testing points $P_j(I_j, V_j, T_j)$, for $j = 1, 2, \ldots, 16$, randomly spread over the temperature interval of 30–55 °C and the voltage interval of 0.1–0.4 V are measured, again with the methanol fuel at 5 vol.% concentration. By substituting $V_u = V_j$, $T_u = T_j$ and a_5 into Eq. (7), one can obtain current value $\tilde{I}_j$ of the projection point Q_j on S_5. If $\tilde{I}_j = I_j$, it indicates that P_j is on the CCS S_5 that satisfies the definition of CCS. Fig. 3 shows the CCS S_5 and the 16 testing points, where symbols '◯' and '+' represent P_j and Q_j, respectively. The deviations between P_j and Q_j, defined as $(\tilde{I}_j - I_j)/I_j \times 100\%$, are depicted in Fig. 4. It turns out that all the deviations of the testing points are less than 5%, thus sufficiently validating the notion of CCS.

4.2. Establishment of CCSs and feasible measurement regions

Following a similar procedure that creates S_5, the other five CCSs corresponding to the concentration levels listed in Table 1 are established. The experimental results show that CCSs may intersect with each other due to the inherent characteristics of a DMFC. Such a situation will lead to ambiguities in the ICCS algorithm, hence the feasible regions of concentration and voltage should be well defined.

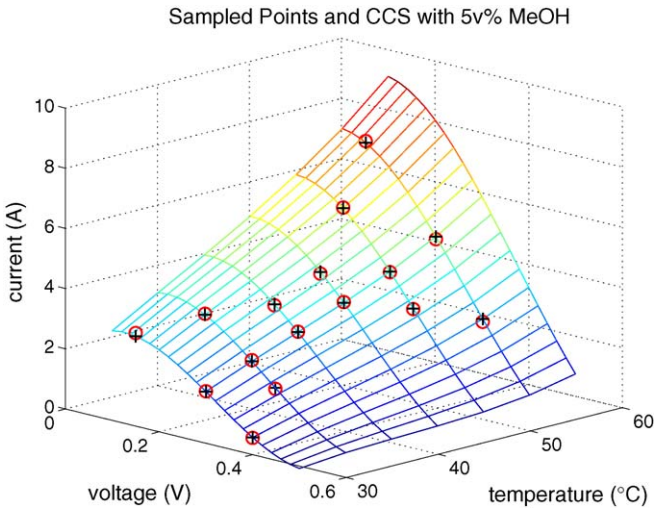

Fig. 3. Pre-established CCS S_5, individually sampled points P_j, and the projection points Q_j with the same concentration level (5 vol.%).

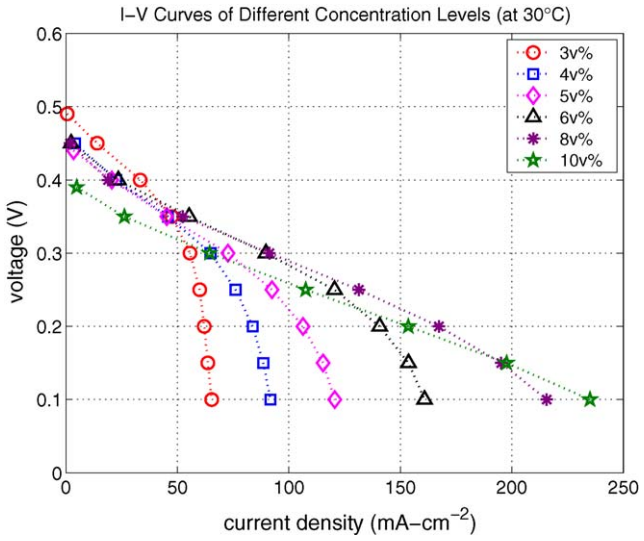

Fig. 5. The *I–V* curves of different concentration levels (at 30 °C).

First, the *I–V* curves with different concentration levels are depicted in Fig. 5 (at 30 °C). It shows that all the curves intersect with each other near the region of higher voltage (or lower current density). Meanwhile in the so-called mass transport or concentration losses region (generally at lower voltages), the *I–V* curves spread out by the increase of concentration in an ordered manner. As a result, it is less to employ the estimation algorithm in the lower voltage region less than 0.35 V to avoid ambiguities and achieve increased accuracy in the results. However, owing to efficiency consideration, it is not advisable to operate a DMFC below the lower voltage region. Consequently, for a larger-scale DMFC system, it is suggested that a sensor unit is included separate from the fuel cell stack that generates electricity. The two parts can operate independent at different voltage intervals. As for a smaller-scale DMFC system, to simplify the system architecture, a sensor-less approach can be used. The fuel cell operates at a higher voltage in the normal state. Whenever the concentration information is needed, the energy management system lowers the voltage of the fuel cell to acquire the necessary measurement data, and then returns to the normal state. In the present example, the time required for taking a stabilized measurement point $P_u(I_u, V_u, T_u)$ is about 2–6 s.

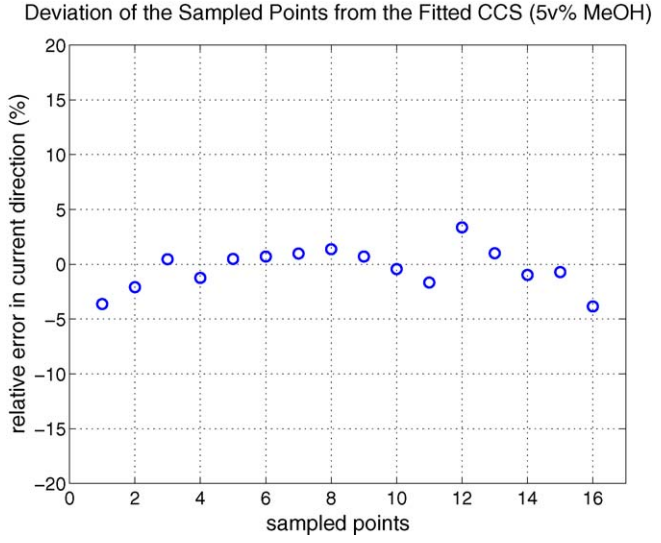

Fig. 4. Relative error (deviation between P_j and Q_j) in current direction regarding the CCS S_5.

Fig. 5 also reveals that when the concentration is within the region of 3–8 vol.%, the *I–V* curves spread out with increase of concentration in an ordered manner. However, when the concentration is further increased to 10 vol.%, the curve intersects the others and shows a tendency to move 'backward'. This is mainly due to the methanol crossover phenomenon and can become more significant at higher temperatures. Accordingly, the feasible region of the measured concentration should be confined within a certain range. In the present example, it should not exceed 8 vol.% (2.0 M). Fortunately, in a practical DMFC system, methanol crossover should be properly suppressed to ensure adequate fuel utilization efficiency and Faradaic efficiency. The literature has indicated that the suggested fuel concentration would be less than 1.5–2.0 M (6–8 vol.%) [18,19]. In the following illustration, the methanol concentration will be confined to 3–6 vol.% while the corresponding CCSs are shown in Fig. 6.

The above limitations are derived by the inherent characteristics of a DMFC. All the electrochemical type methanol sensors will more or less suffer from similar situations. The feasible regions depend on the MEA design of a fuel cell system. For example, a membrane coated with a thin palladium (Pd) film will dramatically reduce the methanol crossover phenomenon [5], thus extending the range of the measured concentration. In such a situation, the present ICCS algorithm will also possess a larger measurement domain. Furthermore, if other measurement indices are chosen as the basis of $\Re^3$, the ranges of the measurement practice may then have corresponding changes.

4.3. Evaluation of ICCS algorithm

To evaluate the proposed ICCS algorithm, three additional concentration levels (shown in Table 1) are introduced to serve

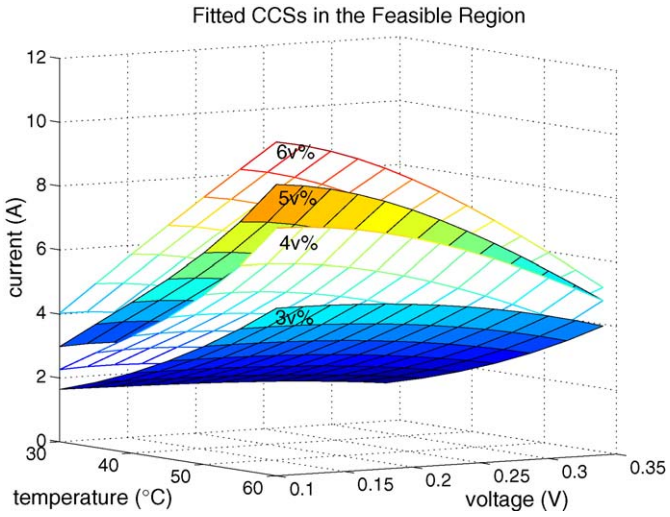

Fig. 6. The CCSs in the feasible region that guarantees the ICCS algorithm to have a unique and robust estimation.

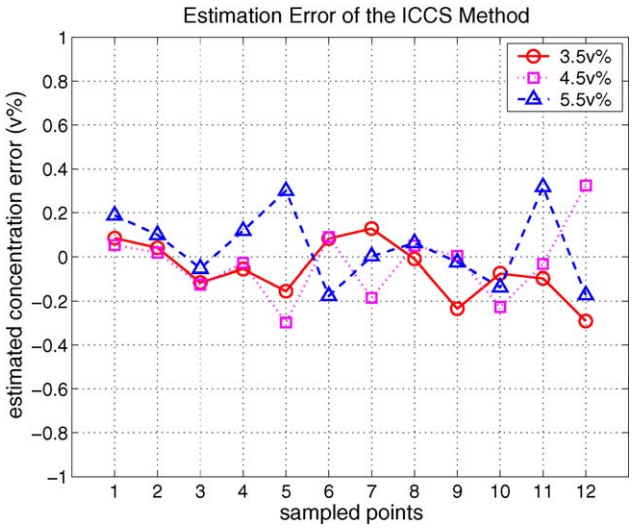

Fig. 8. The evaluation of the proposed ICCS algorithm $\Re^3$.

as the unknown concentration to be estimated. Each of the three levels is assigned 12 measured points randomly in the temperature range from 30 to 55 °C with a 5 °C increment, and the voltage range from 0.1 to 0.3 V with a 0.05 V increment. The distribution of the 36 testing points in the three-dimensional measurement space $\Re^3$ is shown in Fig. 7. Since there are four pre-established CCSs (in Fig. 6), the ICCS algorithm will have a 3rd ordered estimation when adopting Eqs. (7) and (8). The results are shown in Fig. 8. It indicates that the estimation is quite robust since all the estimated errors have distributed over a uniform range of ±0.3 vol.% (about ±0.075 M). This is believed to have adequate accuracy for a real application.

In the aforementioned illustration, the proposed approach provides good results under the situations that both the temperature and voltage are varying. Hence it is more suitable for in situ measurement where the impact of the surroundings may influence the operation conditions of the system. Accordingly, the feasibility and accuracy of the proposed strategy are verified.

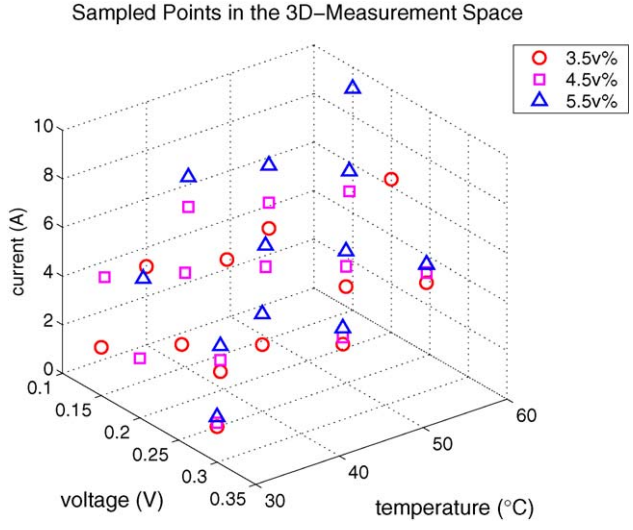

Fig. 7. The distribution of the testing points in the three-dimensional measurement space $\Re^3$.

5. Conclusions

A strategy for estimating the methanol concentration in a DMFC is developed. The approach gives a clear measurement of electrochemical behavior of a DMFC in Eq. (2) by introducing the notion of CCS in a graphical manner. It is also an efficient method to record a set of coefficients depict a CCS in the energy management system of a fuel cell system, instead of the whole experimental database. In practice, the in situ estimation performs only Eqs. (7) and (8) instead of looking table schemes in a multi-dimensional space. Therefore, it is suitable for dynamic operating conditions, taking surrounding influences such as temperature into account.

The primary concept of three-dimensional measurement space and a constant concentration surface have been experimentally verified. The proposed algorithm is shown to possess good results over the range of practical operating conditions. It is also suitable for other kinds of liquid-feed fuel cells where the fuel concentration should be measured. Since the method can be performed in a sensor-less approach that requires none of additional methanol sensors, it is particularly useful for small hand-held applications.

Acknowledgment

This research was financially supported by Antig Technology Co. Ltd. under the project NTIST-93-ME-03 of Northern Taiwan Institute of Science and Technology.

References

[1] Y. Nogami, H. Nunokawa, T. Hirota, US Patent 5,196,801 (1993).
[2] A. Rabinovich, D. Tulimieri, US Patent 6,748,793 (2004).
[3] A. Rabinovich, E. Diatzikis, J. Mullen, D. Tulimieri, US Patent 6,815,682 (2004).

[4] G. Wang, H. Arwin, R. Jansson, IEEE Sens. J. 3 (2003) 739–743.
[5] H.S. Shim, H.J. Ahn, T.Y. Seong, K.W. Park, Electrochem. Solid State Lett. 8 (2005) A277–A278.
[6] G. Luft, G. Starbeck, US Patent 5,624,538 (1997).
[7] X. Ren, S. Gottesfeld, US Patent 6,488,837 (2002).
[8] T. Kumagai, T. Horiba, T. Kamo, S. Takeuchi, K. Iwamoto, K. Kitami, K. Tamura, US Patent 4,810,597 (1989).
[9] W.P. Acker, M.S. Adler, S. Gottesfeld, US Patent 6,824,899 (2004).
[10] J. Zhang, K.M. Colbow, A. Wong, B. Lin, US Patent 6,698,278 (2004).
[11] S.A.C. Barton, B.L. Murach, T.F. Fuller, A.C. West, J. Electrochem. Soc. 145 (1998) 3783–3788.
[12] S.R. Narayanan, T.I. Valdez, W. Chun, Electrochem. Solid State Lett. 3 (2000) 117–120.
[13] S.R. Narayanan, W. Chun, T.I. Valdez, US Patent 6,306,285 (2001).
[14] Z. Qi, C. He, M. Hollett, A. Attia, A. Kaufman, Electrochem. Solid State Lett. 6 (2003) A88–A90.
[15] J.H. Shim, I.G. Koo, W.M. Lee, Electrochem. Solid State Lett. 8 (2005) H1–H5.
[16] J. Larminie, A. Dicks, Fuel Cell Systems Explained, John Wiley and Sons, New York, 2002, pp. 40–53.
[17] R.L. Burden, J.D. Faires, Numerical Analysis, 6th ed., Brooks/Cole Publishing Company, New York, 1997, pp. 107–119.
[18] R. Jiang, D. Chu, J. Electrochem. Soc. 151 (2004) A69–A76.
[19] J.G. Liu, T.S. Zhao, R. Chen, C.W. Wong, Electrochem. Commun. 7 (2005) 288–294.